

Identification of Mesenchymal Stem Cells in Perinodular Fat and Skin in Dupuytren's Disease: A Potential Source of Myofibroblasts with Implications for Pathogenesis and Therapy

Syed Amir Iqbal,^{1,*} Christopher Manning,^{1,*} Farhatullah Syed,¹ Venkatesh Kolluru,¹ Mike Hayton,² Stewart Watson,³ and Ardeshir Bayat^{1,3,4}

Dupuytren's disease (DD) is a fibroproliferative disorder characterized by aberrant proliferation of myofibroblasts, the source of which remains unknown. Recent studies indicate that circulating and tissue-resident mesenchymal stem cells (MSCs) can differentiate into myofibroblasts. Therefore, the aim of this study was to profile MSCs from phenotypically distinct DD sites including cord, nodule, skin overlying nodule (SON), and perinodular fat (PNF) compared with unaffected internal controls, that is, distant palmar fat (DPF) and transverse palmar fascia (Skoog's fibers) as well as external control carpal tunnel (CT) tissue including skin, fat, and fascia. Freshly isolated primary fibroblasts as well as cells grown up to passage 5 (P5) from DD ($n=27$) and CT ($n=14$) samples were analyzed for the presence of established MSC markers CD73, CD90, and CD105 and absence of hematopoietic marker CD34 using fluorescence-activated cell sorting, in-cell quantitative western blotting, immunohistochemistry, and immunocytochemistry. Freshly isolated cells from SON, PNF, and cord biopsies had a higher number of CD34⁻73⁺90⁺105⁺ cells compared with Skoog's fibers and CT controls. P3 cells obtained from all DD biopsies compared with CT samples differentiated into osteocytes, adipocytes, and chondrocytes. P3 cord and nodule cells expressed intense α -smooth muscle actin staining compared with skin and fat cells. Stem cell markers including stem cell factor, MSC-homing marker CXCR4, and Wnt/ β -catenin downregulator Dkk-1 were all upregulated in SON and PNF compared with CT skin and CT fat, respectively, as shown by real-time quantitative polymerase chain reaction. However, osteogenic marker *OSF-1* had a significantly higher expression in the PNF ($P=0.002$) and cord ($P=0.01$) compared with the nodule. In conclusion, we have shown the presence of MSCs in specific DD tissue phenotypes compared with internal and external control tissue. **These findings provide preliminary support for a potential alternative source of disease myofibroblasts originating from sites such as SON and PNF as opposed to palmar fascia alone.**

Introduction

DUPUYTREN'S DISEASE (DD) IS a common fibroproliferative disorder characterized by progressive, irreducible digital flexion contractures [1]. It has been reported that around 25% of men older than 60 years and of Northern European extraction are affected by DD [2]. DD often starts with a small painless nodule in the connective tissue (fascia) of the palm that eventually develops into a cord-like band that prevents full exten-

sion of the finger [3,4] (Fig. 1). This restriction can severely limit hand function and, consequently, has a significant impact on the patients' quality of life. A lack of clear understanding of the causative factors leading to DD and its exact pathogenesis has meant that an absolute confidence in the best treatment option remains limited. This is evident in the number of different treatment options that are available, such as regional fasciectomy, total fasciectomy, dermofasciectomy, needle fasciectomy, and collagenase injection [1,5–7]. Fasciectomy is the

¹Plastic and Reconstructive Surgery Research, Manchester Interdisciplinary Biocentre, University of Manchester, Manchester, United Kingdom.

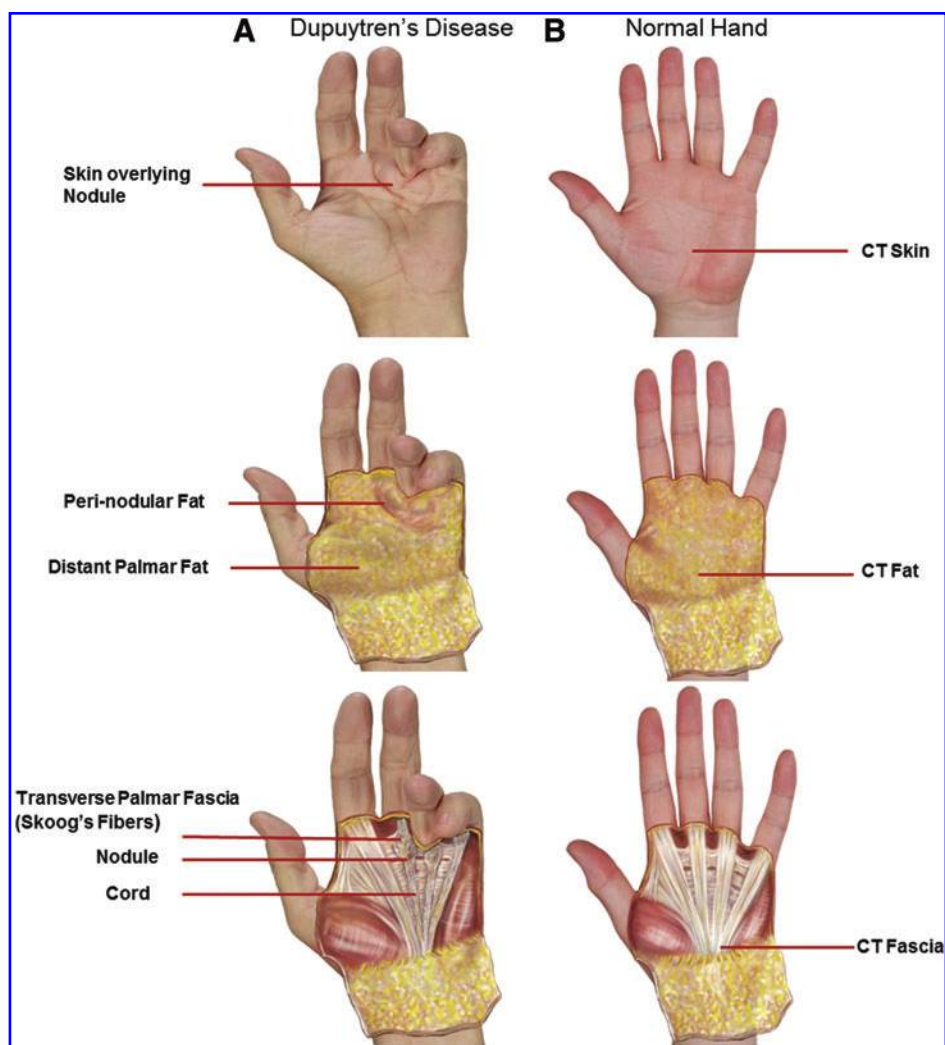
²Department of Hand and Upper Limb Surgery, Wrightington Hospital, Wrightington, United Kingdom.

³Department of Plastic and Reconstructive Surgery, South Manchester University Hospital Foundation Trust, Wythenshawe Hospital, Manchester, United Kingdom.

⁴School of Translational Medicine, University of Manchester, Manchester, United Kingdom.

*These authors contributed equally to this work.

FIG. 1. Photograph of Dupuytren's contracture compared with normal hand. (A) Palmar view of Dupuytren's contracture at advanced stage; (B) normal hand. CT, carpal tunnel. Color images available online at www.liebertonline.com/scd



most common surgical procedure (involving excision of the diseased fascia alone) carried out for treatment of DD, but it is associated with a high rate of recurrence pointing toward a possible source of cells that may be implicated in disease etiology and recurrence [4].

The main cell type responsible for DD is thought to be the myofibroblasts that are derived from the resident fibroblasts in normal fascia [8,9]. In DD, skin overlying nodular (SON) tissue as well as perinodular fat (PNF) have been shown to be abnormal and it has been suggested that they may have a role in the pathogenesis of DD [10–12]. The reduced rate of recurrence after a dermofasciectomy (a surgical procedure that involves excision of the SON and PNF including the nodule and cord en bloc) also demonstrates that the skin and fat in DD may be involved in the disease process [13]. Although the involvement of the skin in DD is not a new concept [10], more understanding of its function in terms of disease progression and recurrence would be most beneficial.

The recruitment of progenitor cells from surrounding areas and their differentiation into myofibroblasts are not peculiar to DD. Hepatic stellate cells differentiate to myofibroblasts in the liver [14] and epithelial-mesenchymal transition provides another mechanism to generate myofibroblasts in pulmonary and renal fibrosis [15,16]. In addition, it is suggested that fibrocytes that circulate in the blood migrate to

tissue and differentiate into myofibroblasts as shown in lung fibrosis [17]. Recently, it has been shown that carcinoma-associated fibroblasts are derived from bone marrow mesenchymal stem cells (MSCs) [18]. Moreover, both skin and fat tissues have been cited as sources of MSCs in humans [19,20]. Potentially, MSCs located in the SON and PNF have the ability to differentiate into myofibroblasts that could contribute to the excessive contractile fibrotic process that is considered to be the hallmark of DD pathogenesis.

We previously showed that a pool of hematopoietic stem cells (HSCs) and MSCs were present in the skin, fascia, and fat isolated from DD tissue [21]. In that previous study, we identified MSCs on the basis of single-color fluorescence-activated cell sorting (FACS), utilizing cell surface markers that included CD13, CD29, CD44, CD90, and CD166 without confirmation using a differentiation assay. To further characterize and functionally verify the MSCs implicated in DD, we have adopted the currently accepted criteria for identifying MSCs established by the International Society for Cellular Therapy (ISCT) [22]. The ISCT criteria identify MSCs as “plastic adherent” when maintained in standard culture conditions and that MSCs must express CD105, CD73, and CD90, and lack expression of CD45, CD34, and CD14 surface molecules. In addition, MSCs must differentiate to osteoblasts, adipocytes, and chondroblasts in vitro [22].

Therefore, this study aims to identify and characterize MSCs using multicolor FACS in DD tissue phenotypes including cord, nodule, PNF, DFP, and SON compared with control internal and external tissue based on the ISCT recommendations. We will then assess the expression of key stem cell-related and migratory genes as well as functionally assess the progenitor potential of MSCs by using *in vitro* culture assays.

Materials and Methods

Patient data

This study was carried out in accordance with the Declaration of Helsinki and has been approved by the NHS national research ethics committee. All tissues were collected after patients had given informed consent before their operation at University Hospital of South Manchester, Wythenshawe Hospital in Manchester, and Wrightington Hospital in Wrightington, England, United Kingdom (see Supplementary Table S1 for DD patient data; Supplementary Data are available online at www.liebertonline.com/scd).

Collection of DD and CT biopsies

Biopsies of cord, nodule, PNF, and SON were obtained from patients undergoing routine (standard for our practice) fasciectomy surgery for Dupuytren's disease ($n=27$; age range: 47–80 years; mean age=65 years; 26 males and 1 female). Skoog's fibers (transverse palmar fascia) and distant palmar fat (DPF) taken 2 cm from the margin of the diseased tissue were also obtained as internal controls. In addition to the internal controls, external control tissue samples of skin, fat, and transverse carpal ligamentous fascia were obtained from patients undergoing carpal tunnel (CT) open surgical release ($n=14$; age range: 44–80 years; mean age=59 years; all female). Before being enrolled in the study, patients undergoing CT release were screened for DD, family history of DD, or any associated condition, based on a personal interview, proforma assessment, and clinical examination. All samples were collected and placed in Dulbecco's minimal essential medium (DMEM; PAA) in 10% neutral buffered formalin (Sigma-Aldrich) and in RNAlater (Ambion; refer to Supplementary Fig. S1 for details).

Isolation and culturing of primary cells from tissue biopsies

All tissue biopsies were placed in complete media, that is, DMEM supplemented with 10% fetal bovine serum (FBS), 2 mM glutamine (PAA), 100 $\mu\text{g}/\text{mL}$ penicillin/streptomycin, and 0.1 mM nonessential amino acids (Sigma-Aldrich), and were washed thoroughly in phosphate-buffered saline (PBS; PAA) before being minced and incubated in collagenase A (10 mg/mL; Roche Diagnostics) for 5 h in the water bath at 37°C. The suspension was passed through a 70- μm cell strainer (BD Biosciences) to remove any remaining tissue. Cells were then washed once with PBS and then either resuspended in 5 mL of complete medium for cell culture or passed through a nylon mesh filter (50 μm Filcon; BD Biosciences) to be immediately used as fresh cells for FACS analysis and real-time quantitative polymerase chain reaction (RT-qPCR). Cells were maintained in culture up to passage 5 (P5) and media was fed to cultures every 3–5 days.

FACS analysis

Multicolor FACS analysis was performed as described earlier [23]. Briefly, freshly isolated cells from tissue biopsies or P0–P5 cells were trypsinized and washed once with Hank's Balanced Salt Solution (PAA); 100 μL of primary antibodies (1:20 dilution) conjugated to fluorophores against human cell surface markers CD34, CD73, CD90, and CD105 (Table 1) were added to the pellet and incubated on ice for 30 min. Appropriate isotype controls were used along with negative controls. Sytox blue (Invitrogen) was added to determine viable cells in the samples analyzed. The samples were analyzed on Dako CyAn ADP flow cytometer (Beckman Coulter) equipped with 4 lasers. To identify CD34⁻73⁺90⁺105⁺ cells, Sytox blue negative cells (viable cells) were gated on CD34 (lowest expressed) versus CD90 (highly expressed) dot plot and cells negative for CD34 and positive for CD90 were further gated on the CD73 versus CD105 dot plot. The necessary color compensation was done during and also after data acquisition.

Real-time quantitative polymerase chain reaction

The expression of characteristic stem cell-related and migratory genes was investigated by RT-qPCR. Freshly isolated cells or P0–P5 cells were collected in Trizol (Invitrogen) and RNA was isolated by Qiagen RNeasy mini kit (Qiagen) as per manufacturer's instructions and quantified on Nanodrop 2000 (Thermoscientific). Complementary DNA was synthesized from 1 μg RNA using qScript (Quanta Biosciences). cDNA was amplified by RT-qPCR using primers as described in Table 2. Each RT-qPCR was carried out with a total volume of 10 μL in each well of a 96-well plate. This comprised of 5 μL of MasterMix (Roche Diagnostics), 0.1 μL of forward primer, 0.1 μL of reverse primer, 0.1 μL of probe from the Universal Probe Library (Roche Diagnostics), 2.7 μL of nuclease-free water (Ambion), and 2 μL of cDNA (normalized to 10 ng/ μL). All reactions were carried out in triplicate.

MSC differentiation assay

To determine whether the cells grown from DD and CT biopsies were uncommitted MSCs capable of differentiating into adipogenic, osteogenic, and chondrogenic lineages, we grew P3 cells in lineage-specific StemPro adipogenic, chondrogenic, and osteogenic media (Invitrogen). Briefly, cells were washed once in PBS and resuspended at a concentration of 1.6×10^7 cells/mL in complete media. For chondrogenic pathway, 5 μL of the cell suspension was spotted on the

TABLE 1. ANTIBODIES AND CONJUGATED FLUORESCENT PROBES USED FOR FLUORESCENCE-ACTIVATED CELL SORTING

Surface marker	Fluorescent molecule	Emission wavelength (nm)
CD34	FITC	519
CD73	APC	660
CD90	PerCP-Cy5.5	678
CD105	PE	578

FITC, fluorescein isothiocyanate; APC, allophycocyanin; PE, phycoerythrin.

TABLE 2. PRIMER USED IN REAL-TIME QUANTITATIVE POLYMERASE CHAIN REACTION

Gene name	Sequence 5' to 3'	UPL number	GenBank accession number
CXCR4	Left - attgggatcagcatcgact Right - caaactcacaccttgcttg	79	NM_003467
Dkk-1	Left - caggcgtgcaaatctgtct Right - aatgattttgatcagaagacacacata	4	NM_012242
Osf-1	Left - aactgaccaagcccaaacct Right - ggtgacatctttaatccagca	2	NM_002825
Rex-1 (ZPF42)	Left - tctgagtacatgacaggaagaa Right - tctgataggcaatgccaggt	65	NM_174900
SCF	Left - gcgctgcctttccttatg Right - ccttcagttttgacgagagga	68	BC_143899

UPL, Universal Probe Library (Roche Diagnostics).

middle of the 24-well plate wells in triplicates and incubated at 37°C/5% CO₂ for 2 h. A total of 1×10⁴ cells/cm² were added for adipogenic pathway and 5×10³ cells/cm² were added for osteogenic pathway in 24-well plates and incubated at 37°C/5% CO₂ for 2 h, all in triplicates. After 2 h the complete media was removed and replaced with 500 µL respective StemPro media. The media was changed every 3rd day until day 21. Detection of differentiation was done by staining calcium deposited by osteocytes using Alzarin Red S (Sigma-Aldrich); lipid secreted by adipocytes was stained by Oil Red O; chondrocytes were detected by staining sulfated proteoglycans with Alcian blue as described earlier [24].

Immunohistochemistry

The tissue biopsies were embedded in paraffin wax and sectioned into 5-µm sections. We followed the usual immunohistochemistry procedure with antigen retrieval for 30 min in Dako antigen retrieval solution (Dako) at 95°C. After washing with PBS, tissue sections were incubated in blocking buffer (PBS+2% FBS) for half an hour and then incubated in primary mouse anti-human CD34, CD90 (1:100 dilution), CD73, and CD105 (1:200 dilution) antibodies (Abcam) overnight at 4°C. Secondary anti-mouse fluorescein isothiocyanate (FITC)-conjugated (1:250 dilution) antibody (Jackson Laboratories) was added to the sections after thorough washing with PBS and incubated for an hour at room temperature. 4',6-diamidino-2-phenylindole (DAPI) was added to the tissue section for nuclei staining. Isotype-matched antibodies were used as a negative control.

Immunocytochemistry

Cells from P1 to P4 were grown to 80% confluence on 13-mm-diameter cover slips (VWR). Cells were fixed for 1 h in 10% neutral buffered formalin (Sigma-Aldrich). After washing with PBS, cells were incubated in Odyssey blocking buffer (LI-COR Biotechnology, UK Ltd.) for 30 min and then incubated in primary mouse anti-human α-smooth muscle actin (α-SMA), CD34, CD73, CD90, and CD105 (all 1:200 diluted in PBS except α-SMA; 1:1,000) antibodies (all from Abcam) overnight at 4°C after washing with PBS. Cells were labeled by secondary anti-mouse FITC-conjugated (1:250 dilution) antibody (Jackson Laboratories) after thorough washing with PBS and incubated for 1 h at room temperature. DAPI was added to stain nuclei.

In-cell western blotting

P3 DD-derived cells of all tissue sites were grown to 90% confluence in T25 flasks. Cells were trypsinized and counted on Accuri C6 flow cytometer (Accuri Cytometers); 1×10⁴ cells per well were plated in 96-well plates (Corning) in triplicates and grown in complete media for up to 48 h at 37°C/5% CO₂. The cells were then fixed in 10% neutral buffered formalin for 1 h at room temperature. The wells were washed 3 times with PBS (150 µL/well), permeabilized with PBS/0.1% Triton X-100 (150 µL/well, 3 times, 5 min each; Sigma-Aldrich), and blocked in Odyssey blocking buffer (LI-COR; 150 µL/well) for 2 h at room temperature. The samples were then incubated with mouse anti-human-CD34, -CD73, -CD90, and -CD105 antibodies (1:100 for optimal signal-to-noise ratio; Abcam) in Odyssey blocking buffer (LI-COR) overnight at 4°C temperature (50 µL/well) and subsequently washed with PBS/0.1% Tween-20 (150 µL/well) 3 times. Infrared rabbit anti-mouse IR-Dye800CW secondary antibody (1:800; LI-COR) in PBS/0.5% Tween-20 were then added (50 µL/well). The plates were incubated for 1 h at RT, and the wells were washed with PBS/0.1% Tween-20 3 times. The plates were imaged on an Odyssey infrared scanner (LI-COR) using the microplate 2 setting with sensitivity of 7.5 in the 800 nm wavelength channel. Data were acquired using Odyssey software and exported and analyzed in Excel (Microsoft). All values obtained from primary antibodies treatment were background subtracted from wells treated only with secondary antibody.

Statistical analysis

The percentage of cells positive for each individual MSC marker (CD34, CD73, CD90, and CD105) was determined using Summit v4.3 (Dako). Five-color FACS was performed to find the percentage of CD34⁻CD73⁺CD90⁺CD105⁺ cells. Gene expression was analyzed using the 2^{-ΔΔCt} method [25] and REST 2009 software was used to test the statistical significance of the differences in gene expression [26]. A *P* value of <0.05 was considered statistically significant. Both RT-qPCR and FACS data were analyzed in a pairwise method (ie, cord compared with CT fascia, nodule compared with CT fascia, cord compared with nodule, SON compared with CT skin, PNF compared with CT fat, and DPF compared with CT fat) and an unpaired 2-tailed *t*-test was used to check the statistical significance of the results using GraphPad Prism version

5.00 for Windows, GraphPad Software (www.graphpad.com). Multicolor FACS data from different passages were analyzed by comparing means through one-way ANOVA with Dunnett's post-test using GraphPad Prism version 5.00.

Results

FACS-based characterization of DD- and CT-derived cells

FACS analysis showed that fresh cells from cord, nodule, PNF, and SON were more positive for MSC markers CD73,

CD90, and CD105 compared with their respective CT controls (Fig. 2A). In addition, cells from cord, nodule, and SON were also significantly more positive for CD34 compared with control tissue (Cord, $P=0.01$; Nodule, $P=0.02$; and SON, $P=0.0009$). All other samples were negative for CD34. The expression of CD73, CD90, and CD105 increased with passage up to P5 when all cultured cells showed a similar high expression of all 3 markers. CD34 expression reduced in levels from fresh cells to P5 in all samples (Supplementary Table S2).

Fresh cells from PNF were significantly more positive than CT fat for MSC markers CD73 (31.1% vs. 7.7%, $P=0.03$) and

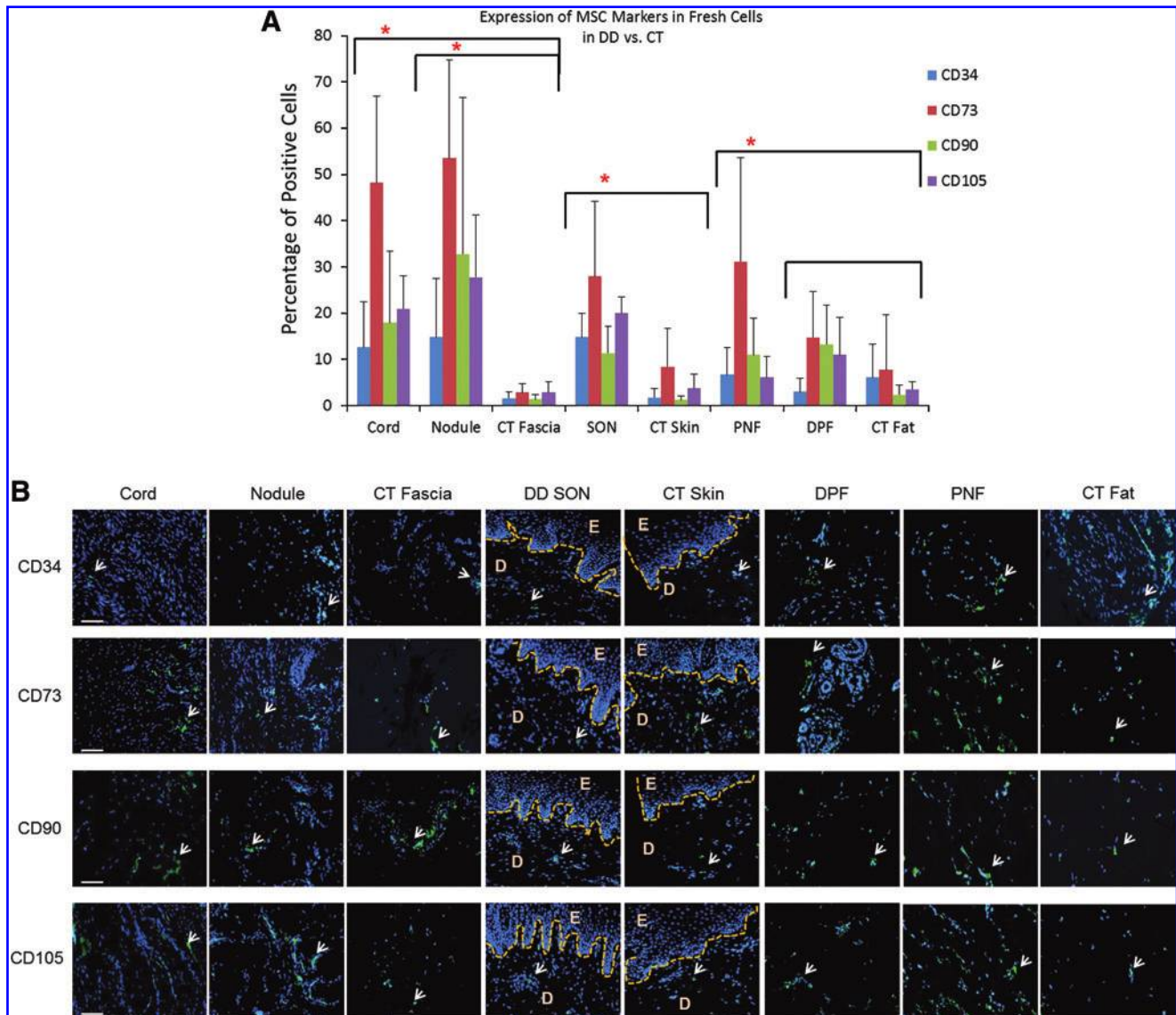


FIG. 2. Single-color FACS analysis of freshly isolated cells from Dupuytren's and carpal tunnel biopsies. (A) The percentage of cells positive for CD34, CD73, CD90, and CD105 markers in diseased tissue and external control. DD nodule and cord showed overall higher expression of all markers compared with external control CT fascia. Same was true for DD skin over nodule compared with CT skin and PNF compared with CT fat. Data shown are from 10 DD and 6 CT patients ($*P < 0.05$). (B) Immunohistochemistry showing the expression of CD34, CD73, CD90, and CD105 (white arrows) in DD and CT biopsies. All fat samples from DD and CT showed higher expression of CD34 compared with other biopsies. Epidermis from skin over nodule and CT skin showed no expression of any of the markers, confirming their presence in dermis alone. D, dermis; DD, Dupuytren's disease; E, epidermis; CT, carpal tunnel; DPF, distant palmar fat; PNF, perinodular fat; SON, skin over nodule; FACS, fluorescence-activated cell sorting. Scale bar = 100 μ m. Color images available online at www.liebertonline.com/scd

CD90 (11% vs. 2.35%, $P=0.02$), whereas CD105 expression was higher in PNF (6.1% vs. 3.5%, $P=0.09$), although this was not statistically significant. The expression of CD34 was similar in PNF and CT fat (6.7% vs. 6.1%; Fig. 2A). The expression of all the above markers was investigated up to P5 and it was found that the expression of CD73, CD90, and CD105 was increased in all samples and became uniform by P5 (Supplementary Table S2).

When we compared fresh cells from DPF to CT fat, we found more expression of MSC markers in DPF than CT fat (Fig. 2A); however, the higher expression was not statistically significant ($P=0.09$). On the other hand, DPF and PNF showed similar expression of MSC markers from P0 to P5 (Supplementary Table S2). CD73, CD90, and CD105 are all highly expressed in the cord and nodule. The expression of CD73, CD90, and CD105 were consistently higher in the nodule compared with cord at each passage. At P0, CD90 was expressed significantly higher in the nodule compared with the cord (92.7% vs. 83.7%, $P=0.04$), as was CD105 (93.3% vs. 80.2%, $P=0.003$). However, the hematopoietic marker, CD34, was significantly higher in the fresh cells derived from the cord compared with the nodule (8.7% vs. 1.2%, $P=0.01$).

As the markers for HSCs (CD34) and MSCs are considered to be solely expressed in the dermis, we looked for their expression in all DD and CT tissue sections and confirmed that, in DD skin and control skin samples, all the markers were expressed in dermis (Fig. 2B). Immunohistochemically, the expression of CD34 and MSC markers was similar between cord and nodule (Fig. 2B), but PNF stained intensely for all markers compared with DPF and CT fat.

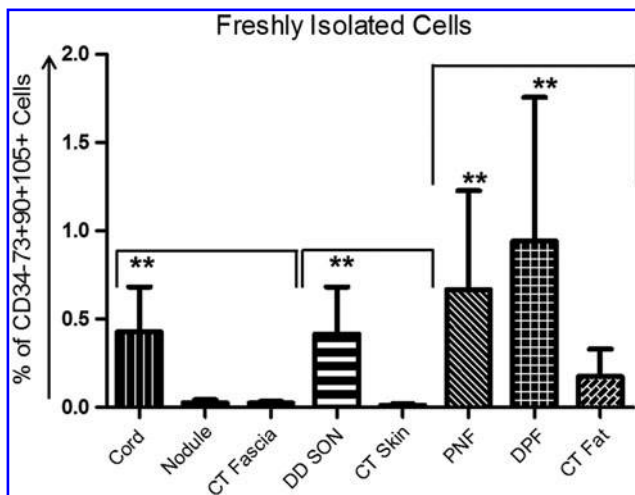


FIG. 3. DD-derived fresh cells show higher expression of CD34⁻73⁺90⁺105⁺ cells compared with external CT control. Freshly isolated cells were labeled with mouse anti-human antibodies against CD34, CD73, CD90, and CD105 antigens. Viable cells (Sytox blue⁻) were selected and gated on CD34 versus CD90 plot. CD34⁻90⁺ cells were then gated on CD73 versus CD105 plot and CD34⁻73⁺90⁺105⁺ cells were selected. Cord, SON, PNF, and DPF contained significantly higher numbers of MSCs compared with their respective CT controls. The gates were set according to the respective isotype control plots for individual fluorophores used. Mean \pm SD shown here represents data from 8 patients (** $P < 0.01$). SD, standard deviation.

To confirm the presence of CD34⁻73⁺90⁺105⁺ MSCs (as per ICST definition), we labeled freshly isolated cells from DD and CT biopsies as well as cells in passage P0–P5 with fluorescent-conjugated mouse anti-CD34, -73, -90, and -105 antibodies simultaneously. We found that all DD samples including the internal control, Skoog's fibers, contained CD34⁻73⁺90⁺105⁺ cells, not only in freshly isolated cells but also in P0–P5. When we compared fresh cells from DD with their respective CT controls, using a pairwise analysis, we found significantly higher expression of CD34⁻73⁺90⁺105⁺ cells in cord compared with CT fascia ($P=0.0001$). Although nodule tissue expressed these cells more than CT fascia, it was found to be not statistically significant ($P=0.39$; Fig. 3). Similarly, DD SON showed higher expression of CD34⁻73⁺90⁺105⁺ cells compared with CT skin ($P < 0.0001$); in addition, PNF ($P=0.009$) and DPF ($P=0.0024$) had more of the MSCs compared with CT fat (Fig. 3).

We did not find any statistically significant difference for the expression of CD34⁻73⁺90⁺105⁺ cells between DD and CT cells when grown in culture. On the other hand, we found a significant increase in CD34⁻73⁺90⁺105⁺ cells in P1–P5 of DD-derived cells compared with fresh cells in all samples except for the internal control Skoog's fibers (Fig. 4). Moreover, SON, PNF, and DPF samples have significantly more MSCs starting from P0 to P5 compared with fresh cells (Fig. 4).

Detection of cell surface markers and α -SMA through immunocytochemistry

Expression of CD34, CD73, CD90, and CD105 was also investigated in passaged cells using immunocytochemistry (ICC) (Fig. 5A). We used cells from P3 for immunostaining and found that the expression of CD73, CD90, and CD105 was similar to the results obtained from single-color FACS analysis. The expression of all MSC markers was highest in the nodule, cord, and PNF compared with their respective controls. To identify myofibroblasts in culture, P3 cells were labeled with α -SMA. We found highest expression of α -SMA in cord-, nodule-, and CT fascia-derived cells compared with skin and fat of both DD and CT samples (Fig. 5A). This is in agreement with a recent study in which fascia appeared to have more myofibroblasts compared with its overlying skin [27].

High-throughput in-cell western blotting and quantitative analysis of MSC markers

To quantify the MSC markers at protein level and to corroborate our FACS results, we further analyzed the expression of these markers using a highly sensitive in-cell western blotting technique. In-cell western analysis showed that the in situ expression of CD34, CD73, CD90, and CD105 in P3 cells was similar to what was identified using the FACS analysis and hence confirmed the FACS data (Fig. 5B). CD90 and CD105 were highly expressed in DD samples compared with CT samples, although we did not find any statistically significant difference ($P=0.11$).

Differentiation potential of DD-derived cells

The differentiation potential of cells from DD as well as CT-derived cells were compared with bone marrow (BM)-derived MSCs. All samples demonstrated capacity to

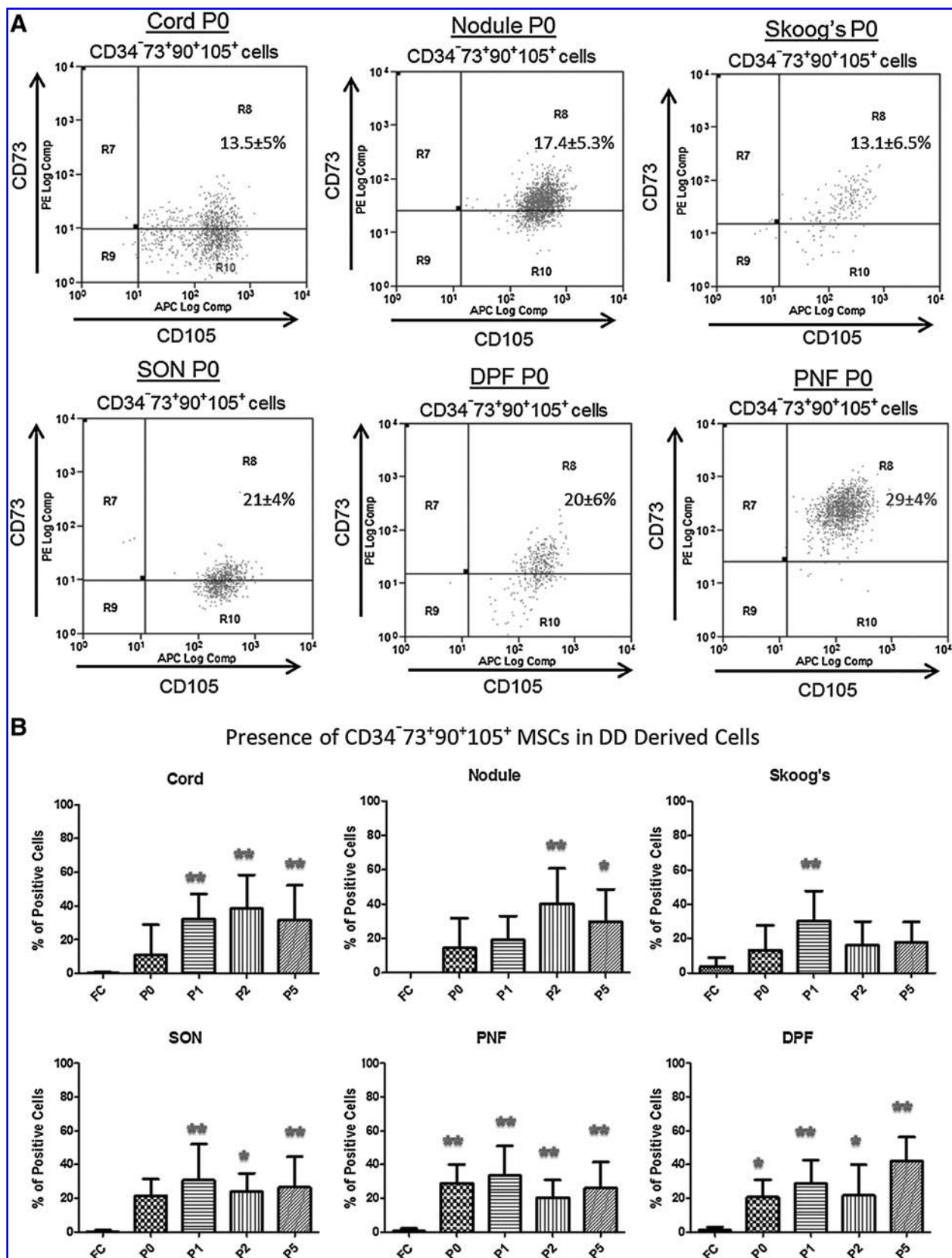


FIG. 4. Multicolor FACS analysis was done to determine the presence of MSCs (CD34⁻73⁺90⁺105⁺) in DD samples. **(A)** DD-derived P0 cells were labeled as described in the legend of Fig. 5. Shown here are mean % ±SD of CD34⁻73⁺90⁺105⁺ cells. Data were pooled from 10 patients. **(B)** Cumulative data from 15 DD and 8 CT patients comparing fresh cells (FC) to P5 cells for CD34⁻73⁺90⁺105⁺ cells. Except for Skoog's fibers (internal control), all other cells showed significant increase in CD34⁻73⁺90⁺105⁺ cells in passages up to P5 (**P* < 0.05, ***P* < 0.01). P0, passage 0 (and so on); MSCs, mesenchymal stem cells.

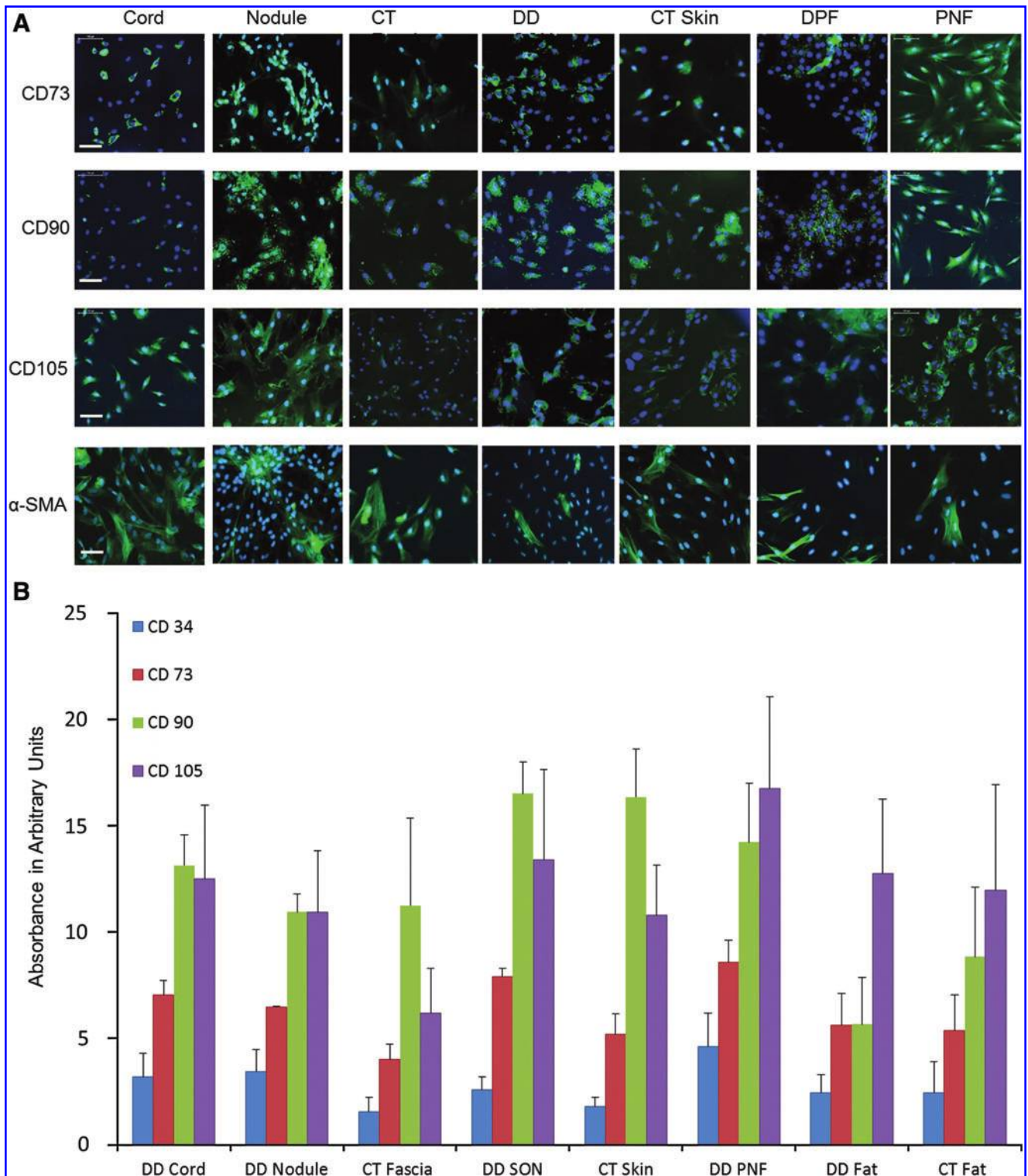


FIG. 5. DD-derived cells (P3) were compared for their expression of MSC markers CD73, CD90, and CD105 against the CT counterparts. **(A)** Nodule, cord, and PNF showed highest levels of expression of all 3 markers compared with CT control, although semiquantitation showed no significant difference (data not shown). The *lower panel* shows the expression of α -SMA in DD- and CT-derived P3 cells. Cord, nodule, and CT fascia showed higher expression of α -SMA compared with skin and fat cells. All cells were labeled with secondary rabbit anti-mouse antibodies conjugated with fluorescein isothiocyanate and nuclei counterstained with 4',6-diamidino-2-phenylindole (DAPI). Scale bar represents 100 μ m. **(B)** Quantitative data from in-cell western blot analysis showing that CD90 is highly expressed in all samples followed by CD105 and CD73, whereas CD34 was not expressed much. Data shown here are from 3 independent experiments and represent samples from 6 DD patients and 3 CT patients. α -SMA, α -smooth muscle actin. Color images available online at www.liebertonline.com/scd

differentiate into osteocytes, chondrocytes, and adipocytes (Fig. 6A). However, the extent of the differentiation varied among the different DD samples compared with CT samples when we performed a semiquantification analysis of the differentiation assay data (Fig. 6B).

Osteogenic differentiation. Osteogenesis was established by staining of calcium deposits by osteocytes using Alizarin Red S. Cord and nodule showed a relatively equal ability to differentiate, and both showed a greater ability to differentiate compared with CT fascia (Fig. 6B). Cells from SON differentiated to a greater extent than normal skin. Differentiation to osteocytes was enhanced in DPF, PNF, cord, and nodule compared with skin from DD as well as skin and fascia from CT.

Chondrogenic differentiation. Chondrocytes were identified by the secretion of ECM rich in sulfated proteoglycans, which were detected by Alcian blue staining in acidic conditions. Overall, the cells from DD and CT samples differentiated more into adipocytes and osteocytes compared with chondrocytes (Fig. 6A). Staining of CT fascia, CT skin, and SON samples was slight and infrequent but was positive.

Adipogenic differentiation. Adipogenesis was indicated by the presence of neutral lipid vacuoles stained red with Oil Red O. The most intensive staining was seen in cells derived from fat samples as expected (Fig. 6A). In particular, cells from PNF showed the highest ability for adipogenic differentiation. The fat droplets appeared larger and were more frequent. The differentiation capacity was low in SON, nodule, and CT skin (Fig. 6B).

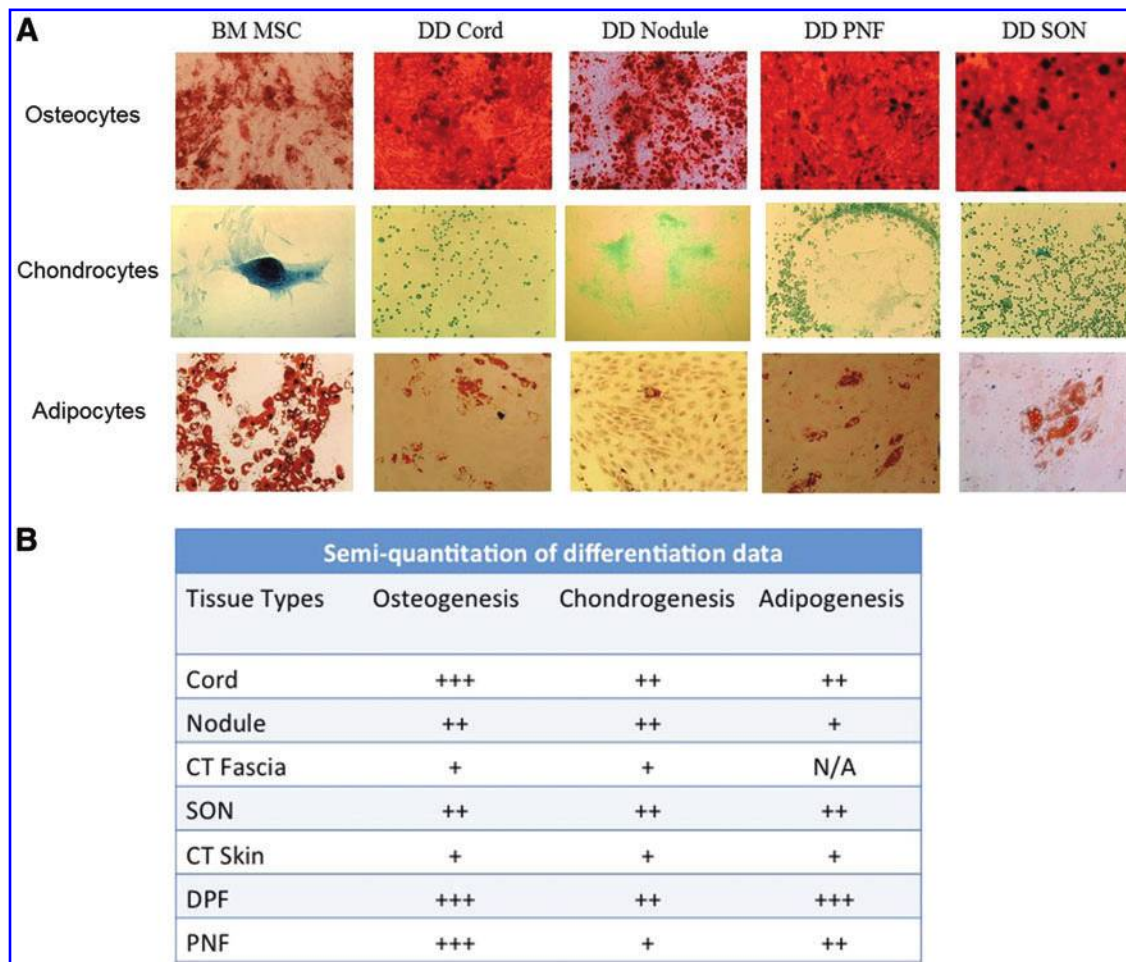


FIG. 6. Trilineage differentiation assay to determine MSC progenitor potential. **(A)** Cells from passage 3 were used to initiate the osteocytic, chondrogenic, and adipogenic pathways in cells derived from DD and BM MSCs. All cells from DD differentiated into the 3 lineages similar to BM MSCs, thus confirming that the biopsies from the DD contained sufficient number of MSCs that could give rise to all 3 lineage cells. **(B)** Quantitation of differentiation assay demonstrating the varying ability of cells to differentiate into 3 mesenchymal lineages. The highest ability for differentiation was seen in cells from PNF differentiating into adipocytes. PNF, along with cord, nodule, and CT fat, also showed a high level of differentiation to all 3 mesenchymal lineages. The lowest ability for differentiation was seen in cells from CT skin and CT fascia. Data quantified by counting stained clusters of Alizarin Red S for osteocytes, Alcian Blue for chondrocytes, and Oil Red O for adipocytes and differentiation capacity of DD and CT cells were compared with bone marrow–derived cells. Data are shown from 3 DD and 3 CT patients. All micrographs were taken at 100× or 200× total magnification. N/A, not applicable, too few samples to make quantitation reliable; + + +, high ability; + +, moderate ability; +, least ability. BM, bone marrow. Color images available online at www.liebertonline.com/scd

Genes involved in MSC homing, maintenance, and early differentiation were found to be upregulated in DD-derived cells

We found that **genes that are involved in MSC homing and differentiation**, that is, *SCF* (stem cell factor), *Osf-1*, *CXCR4*, *Rex-1*, and *Dkk-1*, were **upregulated** in **PNF, DPF, and SON** tissue biopsies compared with control tissue, as shown in Fig. 7A. The increased expression of *SCF* was statistically significant in PNF ($P=0.031$), DPF ($P=0.043$), and SON ($P=0.006$) when compared with their respective CT control biopsies.

A fold change of 2 was shown to be statistically significant for SON in the genes *Osf-1* ($P=0.046$) and *CXCR4* ($P=0.002$). PNF and DPF both showed an increased expression that was statistically significant for *CXCR4* ($P=0.05$ and $P=0.001$) and *Dkk-1* ($P=0.001$). In addition, there was a significantly higher expression of *Osf-1* in PNF ($P=0.002$). The expression of *Rex-1* was also higher in PNF, DPF, and SON in comparison to the control; however, this was not statistically significant.

Only cells derived from PNF and DPF showed high expression of all 5 genes up to P5, although the expression was decreased gradually from P0 to P5 (Fig. 7A, B). In PNF, the expression of *Osf-1* ($P=0.004$) and *Dkk-1* ($P=0.035$) remained significant compared with CT at P5 with a fold change of 5 and 2, respectively. In DPF, only *CXCR4* was expressed significantly higher at P5 compared with control.

SCF, *Osf-1*, *CXCR4*, and *Dkk-1* were expressed significantly more in cord and nodule compared with CT fascia. Compared with CT fascia, *Osf-1* was expressed significantly higher in cord ($P=0.001$) and nodule ($P=0.001$). Further, there was a significantly higher expression of *Osf-1* ($P=0.01$) in the cord compared with the nodule, with a fold change of 7. The expression of *SCF* was significantly higher in the nodule compared with the cord at P0 ($P=0.034$) and P5 ($P=0.025$); the difference was not statistically significant when freshly isolated cells were compared as shown in Fig. 7A.

Discussion

In this study, we have shown the presence and differential distribution of MSCs in cells derived from DD and CT tissue biopsies. In addition, utilizing immunostaining and differentiation assays, we have demonstrated for the first time the morphology and differentiation capacity of these cells as authentic MSCs in DD and compared them with internal and external controls.

In light of the definition given by ICST MSC markers (CD73, CD90, and CD105 positive and CD34 negative) [22], we looked for these markers in freshly isolated cells as well as cells cultured from passage 0 to 5 and found that all of these cells expressed CD73, CD90, and CD105 (Fig. 2 and Supplementary Table S2). CD34 expression was scanty and gradually decreased with every subsequent passage. We further confirmed all our results, first, using immunohistochemistry and ICC (Figs. 2A & 5A) and then by quantifying individual markers utilizing in-cell western blotting (Fig. 5B). The expression levels of the positive MSC markers were found to increase with increasing passage numbers and became more uniform with longer culture times, which is in agreement with existing literature [28]. In contrast, CD34⁺

cells rapidly reduced in number after P0, suggesting that they were less able to attach and proliferate in the culture conditions used for MSC propagation.

There was a higher expression of CD34⁻CD73⁺CD90⁺CD105⁺ cells in SON-, PNF-, and cord-derived fresh cells compared with external control CT (Fig. 3). This finding indicated the presence of more progenitors around the nodule especially in SON and PNF where the cells may possibly originate from and subsequently differentiate into myofibroblasts. The difference in the expression of MSC markers disappeared between DD- and CT-derived cells in vitro, showing that plastic adherence led to selection of cells expressing CD73 and CD90 (Fig. 4).

All cells from passage 3 were differentiated into all 3 lineages of MSCs (Fig. 6A). The ability of cells from DD to differentiate into osteocytes, chondrocytes, and adipocytes fulfills the popular criterion for what constitutes an MSC (Fig. 6B) [22]. The hallmark of myofibroblast recognition is considered to be the expression of contractile fibers staining **α -SMA**. Thus, this was assessed by **immunofluorescence** and we found that cord as well nodule expressed more α -SMA compared with skin and fat (Fig. 5A). Most of the **myofibroblasts are thought to be found in the nodule compared with the cord** [9]; however, we found a similar number of positive α -SMA in both cord- and nodule-derived cells, which may indicate that, in culture, fibroblasts tend to mature into myofibroblasts increasingly.

Despite the extensive number of candidate markers for MSCs, there is no set of markers that is able to specifically identify a homogenous population of MSCs [29]. Some studies have identified CD73 and CD105 to be the most selective MSC markers. In a study that analyzed CD73, CD90, and CD105 in human MSCs, CD73 was proposed to be the most sensitive MSC marker [30]. Adult MSCs were identified by the same stem cell markers used in this study from other pathological tissues such as osteophytes in osteoarthritis [31]. Further, CD73⁺ cells from synovial membranes have shown the ability to differentiate to the same mesenchymal lineages shown in this study [32].

Nevertheless, other studies have shown that MSC populations obtained from different tissues do not differ in their expression of the main set of markers, as used in this study [33]; therefore, the use of selected markers in different types of tissues is considered acceptable. However, **the exact functional role of the surface markers analyzed in MSCs remains unknown**.

We have recently shown that CD34 is expressed in DD tissue [21] and an increase in expression of CD34 has shown to be associated with a higher risk of recurrence in dermatofibrosarcoma protuberans (DFSP) [2,34]. Indeed, **CD34 is known to be expressed on a subset of MSCs known as fibrocytes, which are involved in wound healing**. A study looking at adipose-derived MSCs found that 7.3% of the cells were positive for CD34 [35]. This is in agreement with the relatively low number of PNF cells (6.7%) that were positive for CD34 (Fig. 2A). This percentage markedly declined to <1% by P5 (Supplementary Table S2).

The genes investigated in this study using RT-qPCR have been found to be related to **MSC homing, maintenance, and early MSC differentiation** [36–40]. The statistically significant higher expression of *SCF*, *Dkk-1*, and *CXCR4* in both **SON and PNF** when compared with the corresponding controls

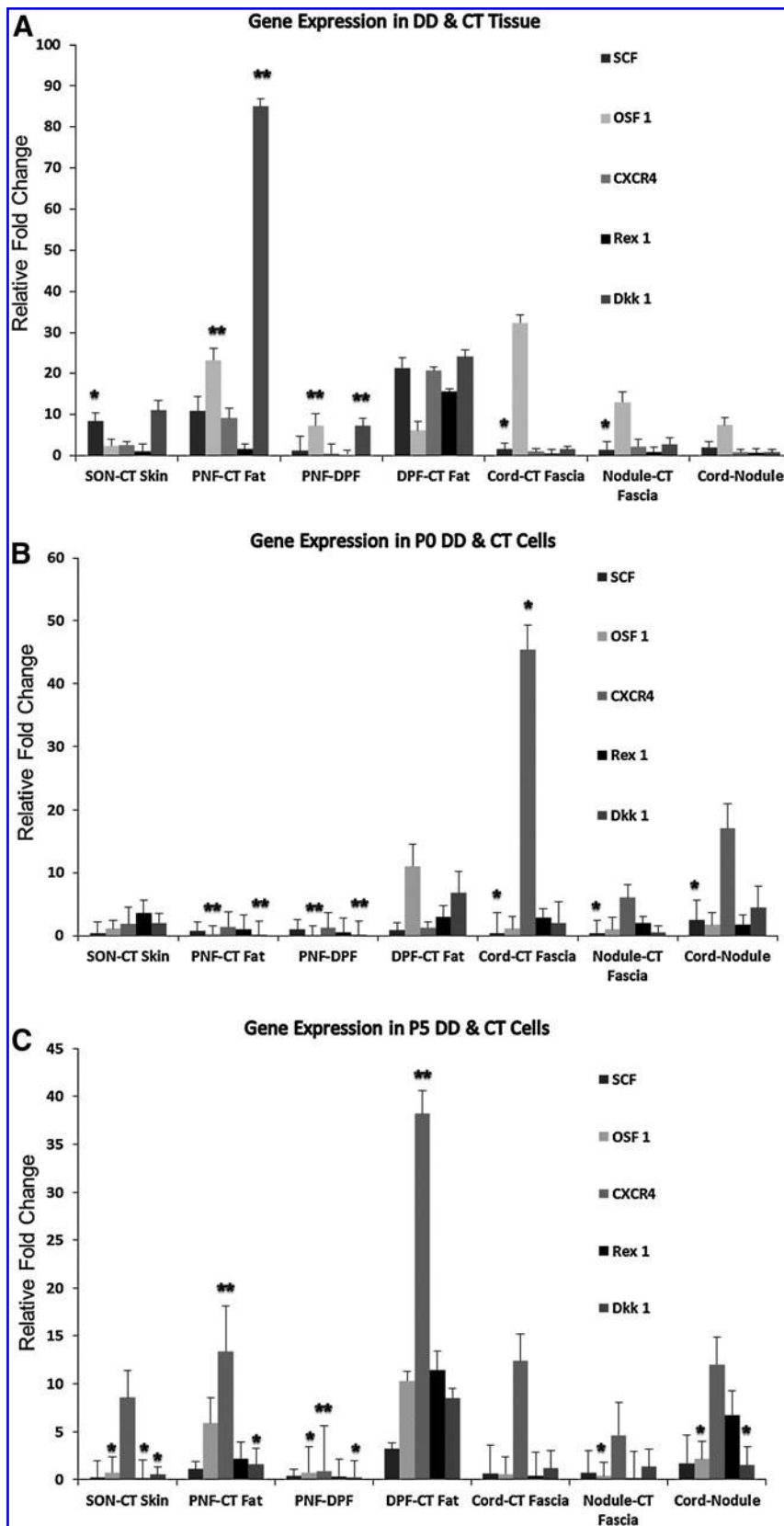


FIG. 7. Quantitative real-time analysis of gene expression from freshly isolated cells (FC) and passages 0 and 5 (P0 and P5) cells. The ΔC_t values for target genes were normalized against the reference gene Rpl32 for each sample (8 patients in total). Data are presented as pairwise relative fold change with respect to the control tissue or otherwise. (A) *SCF* and *Osf-1* were expressed significantly more in DD samples than in CT. Especially cord and nodule expressed significantly more *SCF* compared with CT fascia. (B) At P0, PNF cells expressed significantly more *Osf-1* and *Dkk-1* compared with DPF and CT fat. Cord expressed significantly more *CXCR4* compared with CT fascia as well as *SCF*. (C) At P5, PNF and DPF expressed more of all genes compared with CT fat, but *CXCR4* stands out as the main gene that expressed significantly more in them compared with CT fat (* $P < 0.05$, ** $P < 0.01$). SCF, stem cell factor.

further suggests the presence of an MSC population from these tissues in DD.

SCF is expressed by MSCs [41] and has been cited as a potential marker for proliferation in tumors [42]. The statistically significant higher expression of *SCF* observed in the cord compared with the nodule ($P=0.03$) highlights the possibility that the cord in DD may be a potential site for proliferation of MSCs in this lesion (Fig. 7).

The induction of *Dkk-1* expression is thought to down-regulate the Wnt/ β -catenin pathway in some cancers [43], a pathway that has been shown to be dysregulated in DD [44]. The increased gene expression of *Dkk-1* in the PNF and SON were both statistically significant ($P<0.001$). The association of SON and PNF with a high content of cells expressing stem cell-related genes provides further evidence for their involvement in the pathogenesis of DD. Another important finding was that MSC's homing gene, *CXCR4*, was significantly increased in SON ($P=0.04$) and PNF ($P=0.003$). This gene is highly expressed in breast cancer cells [45] and has a role in the adhesion of prostate cancer cells [46]. *CXCR4* is cited as an adult stem cell marker that is expressed in granulation tissue [47]. Further, *CXCR4*'s role in CD34⁺ fibrocytes migration and hematopoietic cell trafficking through tissue has been verified and may be related to the migration of MSCs in DD [48,49].

PNF showed an increased expression of *Osf-1* ($P=0.002$), a marker of osteoblasts at their earliest stage of differentiation. In a previous gene expression study, *Osf-1* has been shown to be upregulated in DD and Peyronie's disease (PD) [50] (another fibrotic disease associated with DD [51]). Additionally, the authors of this research also stated that PD fibroblast cultures contained pluripotent cells capable of osteogenic differentiation and calcification and suggested that a similar type of cell could be present in DD. Cells of this type located in the cord showed a significantly higher expression of *Osf-1* than the nodule.

Despite the obvious differences in the stem cell gene expression between DD and control CT tissues, the same differences were not seen in cultured cells. As early as P0, the cells seem to lose their expression of *SCF* and *Rex-1*. Other studies have acknowledged this trait in adipose-derived stem cells, wherein *Rex-1* was shown to be expressed only in early passages [38]. This finding represents a stark contrast to MSCs derived from amniotic fluid, wherein expression of *Rex-1* and *SCF* was shown to be present up to passage 20 [52].

In DFSP, expansion of MSCs has been suggested as a cause of the disease alluding to the "tumor stem cell" theory [53]. The MSCs identified in this study may represent "tumor stem cells" in DD. Albeit, the term "tumor" has to be cautiously used, as DD remains a benign condition and at best may be described as a quasi-neoplastic disorder with absence of malignant potential.

Dupuytren's disease has several features in common with a benign neoplastic process, such as the high rate of recurrence after surgery as well as the presence of several chromosomal abnormalities [54,55]. The tumor stem cell hypothesis includes tumors of the mesenchymal lineage in addition to renal, breast, and brain tumors [56]. In addition, a tumor-initiating stem cell population has been identified in human renal carcinomas [57].

In summary, we have shown in this study that freshly isolated cells from DD and CT tissues along with the primary

fibroblasts grown in vitro from passage 0 to passage 5 culture-expanded plastic-adherent cells contain CD34⁻73⁺90⁺105⁺ MSCs. In addition, these cells demonstrate the ability to differentiate into 3 mesenchymal lineages and express stem cell-related genes. Some cells also expressed CD34, an HSC marker that is also expressed by a subset of MSCs called fibrocytes. Further, these results demonstrate that there is a significantly higher number of MSCs present in SON and PNF compared with control that have the phenotypic properties of MSCs in addition to a gene expression profile akin to MSCs. This represents strong evidence for the presence of MSCs in DD tissue.

The results of this research provide preliminary evidence of a potentially alternative source for myofibroblasts present in the hypercellular nodule. DD may not only be a disease of the palmar fascia but also involves SON as well as the perinodular fat. Should this hypothesis be confirmed, specific targeting of these cells could represent an encouraging clinical development.

Acknowledgments

This study was supported by a personal grant from the NIHR (United Kingdom) to A.B. In addition, the authors specially thank the GAT Family Foundation for generous funding and support.

Author Disclosure Statement

None of the authors has any disclosure to declare. No competing financial interests exist.

References

- Shih B and A Bayat. (2010). Scientific understanding and clinical management of Dupuytren disease. *Nat Rev Rheumatol* 6:715–726.
- Hindocha S, DA McGrouther and A Bayat. (2009). Epidemiological evaluation of Dupuytren's disease incidence and prevalence rates in relation to etiology. *Hand (N Y)* 4:256–269.
- Bayat A, EJ Cunliffe and DA McGrouther. (2007). Assessment of clinical severity in Dupuytren's disease. *Br J Hosp Med (Lond)* 68:604–609.
- Bayat A and DA McGrouther. (2006). Management of Dupuytren's disease—clear advice for an elusive condition. *Ann R Coll Surg Engl* 88:3–8.
- van Rijssen AL and PM Werker. (2006). Percutaneous needle fasciotomy in Dupuytren's disease. *J Hand Surg Br* 31:498–501.
- Mavrogenis AF, SG Spyridonos, IA Ignatiadis, D Antonopoulos and PJ Papagelopoulos. (2009). Partial fasciectomy for Dupuytren's contractures. *J Surg Orthop Adv* 18:106–110.
- Wilson GR. (1997). Current surgical treatment of Dupuytren's disease. *Br J Clin Pract* 51:106–110.
- McCann BG, A Logan, H Belcher, A Warn and RM Warn. (1993). The presence of myofibroblasts in the dermis of patients with Dupuytren's contracture. A possible source for recurrence. *J Hand Surg Br* 18:656–661.
- Verjee LS, K Midwood, D Davidson, D Essex, A Sandison and J Nanchahal. (2009). Myofibroblast distribution in Dupuytren's cords: correlation with digital contracture. *J Hand Surg Am* 34:1785–1794.
- Hueston J. (1985). The role of the skin in Dupuytren's disease. *Ann R Coll Surg Engl* 67:372–375.

11. Shih B, JJ Brown, DJ Armstrong, T Lindau and A Bayat. (2009). Differential gene expression analysis of subcutaneous fat, fascia, and skin overlying a Dupuytren's disease nodule in comparison to control tissue. *Hand (N Y)* 4:294–301.
12. Rabinowitz JL, L Ostermann, Jr., FW Bora and J Staefen. (1983). Lipid composition and *de novo* lipid biosynthesis of human palmar fat in Dupuytren's disease. *Lipids* 18: 371–374.
13. Kelly C and J Varian. (1992). Dermofasciectomy: a long term review. *Ann Chir Main Memb Super* 11:381–382.
14. Bataller R and DA Brenner. (2005). Liver fibrosis. *J Clin Invest* 115:209–218.
15. Hinz B, SH Phan, VJ Thannickal, A Galli, ML Bochaton-Piallat and G Gabbiani. (2007). The myofibroblast: one function, multiple origins. *Am J Pathol* 170:1807–1816.
16. Zeisberg M and R Kalluri. (2004). The role of epithelial-to-mesenchymal transition in renal fibrosis. *J Mol Med* 82:175–181.
17. Frid MG, JA Brunetti, DL Burke, TC Carpenter, NJ Davie, JT Reeves, MT Roedersheimer, N van Rooijen and KR Stenmark. (2006). Hypoxia-induced pulmonary vascular remodeling requires recruitment of circulating mesenchymal precursors of a monocyte/macrophage lineage. *Am J Pathol* 168:659–669.
18. Quante M, SP Tu, H Tomita, T Gonda, SS Wang, S Takashi, GH Baik, W Shibata, B Diprete, et al. (2011). Bone marrow-derived myofibroblasts contribute to the mesenchymal stem cell niche and promote tumor growth. *Cancer Cell* 19: 257–272.
19. Toma JG, IA McKenzie, D Bagli and FD Miller. (2005). Isolation and characterization of multipotent skin-derived precursors from human skin. *Stem Cells* 23:727–737.
20. Zuk PA, M Zhu, P Ashjian, DA De Ugarte, JI Huang, H Mizuno, ZC Alfonso, JK Fraser, P Benhaim and MH Hedrick. (2002). Human adipose tissue is a source of multipotent stem cells. *Mol Biol Cell* 13:4279–4295.
21. Hindocha S, SA Iqbal, S Farhatullah, R Paus and A Bayat. (2011). Characterization of stem cells in Dupuytren's disease. *Br J Surg* 98:308–315.
22. Dominici M, K Le Blanc, I Mueller, I Slaper-Cortenbach, F Marini, D Krause, R Deans, A Keating, D Prockop and E Horwitz. (2006). Minimal criteria for defining multipotent mesenchymal stromal cells. The International Society for Cellular Therapy position statement. *Cytotherapy* 8:315–317.
23. Iqbal SA, F Syed, DA McGrouther, R Paus and A Bayat. (2010). Differential distribution of haematopoietic and nonhaematopoietic progenitor cells in intralesional and extralesional keloid: do keloid scars provide a niche for nonhaematopoietic mesenchymal stem cells? *Br J Dermatol* 162:1377–1383.
24. Pittenger MF, AM Mackay, SC Beck, RK Jaiswal, R Douglas, JD Mosca, MA Moorman, DW Simonetti, S Craig and DR Marshak. (1999). Multilineage potential of adult human mesenchymal stem cells. *Science* 284:143–147.
25. Livak KJ and TD Schmittgen. (2001). Analysis of relative gene expression data using real-time quantitative PCR and the 2⁻($\Delta\Delta C_T$) Method. *Methods* 25:402–408.
26. Pfaffl MW. (2001). A new mathematical model for relative quantification in real-time RT-PCR. *Nucleic Acids Res* 29:e45.
27. Verjee LS, K Midwood, D Davidson, M Eastwood and J Nanchahal. (2010). Post-transcriptional regulation of alpha-smooth muscle actin determines the contractile phenotype of Dupuytren's nodular cells. *J Cell Physiol* 224:681–690.
28. Park E and AN Patel. (2010). Changes in the expression pattern of mesenchymal and pluripotent markers in human adipose-derived stem cells. *Cell Biol Int* 34:979–984.
29. Baksh D, L Song and RS Tuan. (2004). Adult mesenchymal stem cells: characterization, differentiation, and application in cell and gene therapy. *J Cell Mol Med* 8:301–316.
30. Haasters F, WC Prall, D Anz, C Bourquin, C Pautke, S Endres, W Mutschler, D Docheva and M Schieker. (2009). Morphological and immunocytochemical characteristics indicate the yield of early progenitors and represent a quality control for human mesenchymal stem cell culturing. *J Anat* 214:759–767.
31. Singh S, BJ Jones, R Crawford and Y Xiao. (2008). Characterization of a mesenchymal-like stem cell population from osteophyte tissue. *Stem Cells Dev* 17:245–254.
32. Arufe MC, AD Fuente, I Fuentes, FJ de Toro and FJ Blanco. (2010). Chondrogenic potential of subpopulations of cells expressing mesenchymal stem cell markers derived from human synovial membranes. *J Cell Biochem* 111:834–845.
33. Musina RA, ES Bekchanova and GT Sukhikh. (2005). Comparison of mesenchymal stem cells obtained from different human tissues. *Bull Exp Biol Med* 139:504–509.
34. Kutzner H. (1993). Expression of the human progenitor cell antigen CD34 (HPCA-1) distinguishes dermatofibrosarcoma protuberans from fibrous histiocytoma in formalin-fixed, paraffin-embedded tissue. *J Am Acad Dermatol* 28:613–617.
35. Zhang Y, GD Zhou, P Yang, S Yin, L Liu de, L Cui, W Liu and YL Cao. (2006). [In vitro study on proliferation and multi-lineage differentiation potential of adipose-derived cells]. *Fen Zi Xi Bao Sheng Wu Xue Bao* 39:152–162.
36. Mukhopadhyay A, DV Do, CT Ong, YT Khoo, J Masilamani, SY Chan, AS Vincent, PK Wong, CP Lim, X Cao, IJ Lim and TT Phan. (2011). The role of stem cell factor and c-KIT in keloid pathogenesis: do tyrosine kinase inhibitors have a potential therapeutic role? *Br J Dermatol* 164:372–386.
37. Yim YS, YH Noh, DH Kim, MW Lee, HW Cheuh, SH Lee, KH Yoo, HL Jung, KW Sung, et al. (2010). Correlation between the immature characteristics of umbilical cord blood-derived mesenchymal stem cells and engraftment of hematopoietic stem cells in NOD/SCID mice. *Transplant Proc* 42:2753–2758.
38. Park E and AN Patel. (2010). Changes in the expression pattern of mesenchymal and pluripotent markers in human adipose-derived stem cells. *Cell Biol Int* 34:979–984.
39. Bhandari DR, KW Seo, KH Roh, JW Jung, SK Kang and KS Kang. (2010). REX-1 expression and p38 MAPK activation status can determine proliferation/differentiation fates in human mesenchymal stem cells. *PLoS One* 5:e10493.
40. Li M, J Yu, Y Li, D Li, D Yan and Q Ruan. (2010). CXCR4+ progenitors derived from bone mesenchymal stem cells differentiate into endothelial cells capable of vascular repair after arterial injury. *Cell Reprogram* 12:405–415.
41. Kim DH, KH Yoo, KS Choi, J Choi, SY Choi, SE Yang, YS Yang, HJ Im, KH Kim, HL Jung, KW Sung and HH Koo. (2005). Gene expression profile of cytokine and growth factor during differentiation of bone marrow-derived mesenchymal stem cell. *Cytokine* 31:119–126.
42. Hirano K, Y Shishido-Hara, A Kitazawa, K Kojima, A Sumiishi, M Umino, F Kikuchi, A Sakamoto, Y Fujioka and H Kamma. (2008). Expression of stem cell factor (SCF), a KIT ligand, in gastrointestinal stromal tumors (GISTs): a potential marker for tumor proliferation. *Pathol Res Pract* 204:799–807.
43. Gonzalez-Sancho JM, O Aguilera, JM Garcia, N Pendas-Franco, C Pena, S Cal, A Garcia de Herreros, F Bonilla and

- A Munoz. (2005). The Wnt antagonist DICKKOPF-1 gene is a downstream target of beta-catenin/TCF and is downregulated in human colon cancer. *Oncogene* 24:1098–1103.
44. Mosakhani N, M Guled, L Lahti, I Borze, M Forsman, V Paakkonen, J Ryhanen and S Knuutila. (2010). Unique microRNA profile in Dupuytren's contracture supports deregulation of beta-catenin pathway. *Mod Pathol* 23: 1544–1552.
 45. Muller A, B Homey, H Soto, N Ge, D Catron, ME Buchanan, T McClanahan, E Murphy, W Yuan, SN Wagner, JL Barrera, A Mohar, E Verastegui and A Zlotnik. (2001). Involvement of chemokine receptors in breast cancer metastasis. *Nature* 410:50–56.
 46. Engl T, B Relja, D Marian, C Blumenberg, I Muller, WD Beecken, J Jones, EM Ringel, J Bereiter-Hahn, D Jonas and RA Blaheta. (2006). CXCR4 chemokine receptor mediates prostate tumor cell adhesion through alpha5 and beta3 integrins. *Neoplasia* 8:290–301.
 47. Patel J, KP Gudehithlu, G Dunea, JA Arruda and AK Singh. Foreign body-induced granulation tissue is a source of adult stem cells. *Transl Res* 155:191–199.
 48. Chamberlain G, J Fox, B Ashton and J Middleton. (2007). Concise review: mesenchymal stem cells: their phenotype, differentiation capacity, immunological features, and potential for homing. *Stem Cells* 25:2739–2749.
 49. Gomperts BN and RM Strieter. (2007). Fibrocytes in lung disease. *J Leukoc Biol* 82:449–456.
 50. Qian A, RA Meals, J Rajfer and NF Gonzalez-Cadavid. (2004). Comparison of gene expression profiles between Peyronie's disease and Dupuytren's contracture. *Urology* 64:399–404.
 51. Waller JI and WC Dreese. (1952). Peyronie's disease associated with Dupuytren's contracture. *J Urol* 68:623–625.
 52. Kim J, Y Lee, H Kim, KJ Hwang, HC Kwon, SK Kim, DJ Cho, SG Kang and J You. (2007). Human amniotic fluid-derived stem cells have characteristics of multipotent stem cells. *Cell Prolif* 40:75–90.
 53. Sellheyer K, P Nelson and D Krahl. (2009). Dermatofibrosarcoma protuberans: a tumour of nestin-positive cutaneous mesenchymal stem cells? *Br J Dermatol* 161:1317–1322.
 54. Wurster-Hill DH, F Brown, JP Park and SH Gibson. (1988). Cytogenetic studies in Dupuytren contracture. *Am J Hum Genet* 43:285–292.
 55. Sergovich FR, JS Botz and RM McFarlane. (1983). Nonrandom cytogenetic abnormalities in Dupuytren's disease. *N Engl J Med* 308:162–163.
 56. Gibbs CP, VG Kukekov, JD Reith, O Tchigrinova, ON Suslov, EW Scott, SC Ghivizzani, TN Ignatova and DA Steindler. (2005). Stem-like cells in bone sarcomas: implications for tumorigenesis. *Neoplasia* 7:967–976.
 57. Bussolati B, S Bruno, C Grange, U Ferrando and G Camussi. (2008). Identification of a tumor-initiating stem cell population in human renal carcinomas. *FASEB J* 22:3696–3705.

Address correspondence to:

*Dr. Ardeshir Bayat
Plastic and Reconstructive Surgery Research
Manchester Interdisciplinary Biocentre
University of Manchester
131 Princess Street
Manchester M1 7DN
United Kingdom*

E-mail: ardeshir.bayat@manchester.ac.uk

Received for publication March 25, 2011

Accepted after revision May 25, 2011

Prepublished on Liebert Instant Online May 25, 2011

This article has been cited by:

1. S. A. Iqbal, G. P. Sidgwick, A. Bayat. 2012. Identification of fibrocytes from mesenchymal stem cells in keloid tissue: a potential source of abnormal fibroblasts in keloid scarring. *Archives of Dermatological Research* . [[CrossRef](#)]
2. Natasha E. Picardo, Wasim S. Khan. 2012. Advances in the understanding of the aetiology of Dupuytren's disease. *The Surgeon* . [[CrossRef](#)]
3. Ivana Ratkaj, Maro Bujak, Davor Juriic, Mirela Baus Loncar, Kreo Bendelja, Kreimir Pavelic, Sandra Kraljevic Pavelic. 2012. Microarray Analysis of Dupuytren's Disease Cells: The Profibrogenic Role of the TGF- β Inducible p38 MAPK Pathway. *Cellular Physiology and Biochemistry* **30**:4, 927-942. [[CrossRef](#)]
4. Latha Satish, William A LaFramboise, Sandra Johnson, Linda Vi, Anna Njarlangattil, Christina Raykha, John Michael Krill-Burger, Phillip H Gallo, David B O'Gorman, Bing Gan, Mark E Baratz, Garth D Ehrlich, Sandeep Kathju. 2012. Fibroblasts from phenotypically normal palmar fascia exhibit molecular profiles highly similar to fibroblasts from active disease in Dupuytren's Contracture. *BMC Medical Genomics* **5**:1, 15. [[CrossRef](#)]